JOURNAL OF THEORETICAL AND APPLIED MECHANICS
54, 2, pp. 517-528, Warsaw 2016
DOI: 10.15632/jtam-pl.54.2.517

THERMAL AND FLUID ANALYSIS ON EFFECTS OF A NANOFLUID OUTSIDE OF A STRETCHING CYLINDER WITH MAGNETIC FIELD USING THE DIFFERENTIAL QUADRATURE METHOD

S.E. Ghasemi
Young Reseachers and Elite Club, Sari Branch, Islamic Azad University, Sari, Iran
e-mail: s.ebrahim.ghasemi@gmail.com

M. Hatami
Department of Mechanical Engineering, Esfarayen University of Technology, Esfarayen, North Khorasan, Iran

Armia Salarian, G. Domairry
Department of Mechanical Engineering, Babol University of Technology, Babol, Iran

In this paper, magnetohydrodynamic flow (MHD) of a nonofluid over a stretching cylinder is investigated numerically. The Differential Quadrature Method (DQM) is applied for solving the governing equations. The influence of relevant parameters such as the magnetic parameter, the solid volume fraction of nanoparticles and the type of nanofluid on the flow, heat transfer, Nusselt number and skin friction coefficient is discussed. Also, comparison with the published results is presented. The results show that the Nusselt number increases with growth in the volume fraction coefficient and Reynolds number but decreases with the magnetic parameter.

Keywords: nanofluids, Differential Quadrature Method (DQM), heat transfer, streching cylinder, magnetic field

1. Introduction

Magnetohydrodynamics can be regarded as a combination of fluid mechanics and electromagnetism, that is, behaviour of an electrically conducting fluid in the presence of magnetic and electric fields. The study of magnetohydrodynamic (MHD) flow has received a great deal of research interest due to its importance in many engineering applications such as plasma studies, MHD power generators, petroleum industries, cooling of nuclear reactors, boundary layer control in aerodynamics and crystal growth (Harada and Tsunoda, 1998; Shang, 2001).

Many investigations have been done on the flow past a moving flat plate or a stretching sheet in the presence of a transverse magnetic field, and a good amount of literature has been generated on this problem (Ishak *et al.*, 2006; Mahapatra and Gupta, 2001).

Examples of such technological applications are hot rolling, wire drawing, glass-fibre and paper production, drawing of plastic films, metal and polymer extrusion and metal spinning (Magyari and Keller, 1999). In all these cases, a study of the flow field and heat transfer can be of significant importance since the quality of the final product depends to a large extent on the skin friction coefficient and the surface heat transfer rate. The heat removal strategies in many engineering applications such as cooling of electronic components rely on natural convection heat transfer due to its simplicity, minimum cost, low noise, smaller size and reliability. In most natural convection studies, the base fluid has a low thermal conductivity, which limits the heat transfer enhancement. However, the continuing miniaturization of electronic devices requires further heat transfer improvements from the energy saving viewpoint (Aminossadati and Ghasemi, 2009). An innovative technique which uses a mixture of nanoparticles and the base fluid was first introduced by Choi (1995) in order to develop advanced heat transfer fluids with substantially higher conductivities. The resulting mixture of the base fluid and nanoparticles having unique physical and chemical properties is referred to as a nanofluid. It is expected that the presence of nanoparticles in the nanofluid will increase the thermal conductivity and, therefore, substantially enhance the heat transfer characteristics of the nanofluid. Convectional heat transfer fluids, including oil, water, and ethylene glycol mixture are poor heat transfer fluids, since the thermal conductivity of these fluids plays an important role in determining the coefficient of heat transfer between the heat transfer medium and the heat transfer surface (Ho *et al.*, 2008).

Mathematical modelling is a vantage point to reach a solution in an engineering problem, so the accurate modelling of nonlinear engineering problems is an important step to obtain accuratre solutions (Zolfagharian *et al.*, 2014a,b,c, 2015; Misagh *et al.*, 2014).

Most differential equations of engineering problems do not have exact analytical solutions, so approximation and numerical methods must be used. Recently, some different methods have been introduced to solving these equations, such as the Variational Iteration Method (VIM) (Ghasemi *et al.*, 2012), Homotopy Perturbation Method (HPM) (Ghasemi *et al.*, 2013; Mohammadian *et al.*, 2015), Parameterized Perturbation Method (PPM) (Ghasemi *et al.*, 2015c), Differential Transformation Method (DTM) (Ghasemi *et al.*, 2014a,c; Hatami *et al.*, 2015), Homotopy Analysis Method (HAM) (Ziabakhsh and Domairry, 2009; Ziabakhsh *et al.*, 2010), Adomian Decomposition Method (Ghasemi *et al.*, 2012), Modified Homotopy Perturbation Method (MHPM) (Ghasemi *et al.*, 2014d), Least Square Method (LSM) (Ghasemi *et al.*, 2014c, 2015b; Darzi *et al.*, 2015), Collocation Method (CM) (Ghasemi *et al.*, 2015a; Atouei *et al.*, 2015), Galerkin Method (GM) (Ghasemi *et al.*, 2015d), and Optimal Homotopy Asymptotic Method (OHAM) (Vatani *et al.*, 2014; Valipour *et al.*, 2015). Also, the Differential Quadrature Method (DQM) is a numerical technique for solving differential equations. It was first developed by Bellman *et al.* (1972). Afterwards, it was improved by Shu (2000). The magnetohydrodynamic natural convection boundary-layer flow on a sphere in a porous medium was studied numerically using the Differential Quadrature Method (DQM) by Moghimi *et al.* (2011). The boundary-layer natural convection flow on a permeable vertical plate with thermal radiation and mass transfer was investigated when the plate moved in its own plane by Talebizadeh *et al.* (2011). They solved the governing equations by means of an excellent analytical method called Homotopy Analysis Method (HAM) and a higher-order numerical method, namely the Differential Quadrature Method (DQM). Hatami and Ganji (2014) applied the Differential Transformation Method with the Padé approximation (DTM-Padé) and the Differential Quadrature Method (DQM) for the motion of a particle in a forced vortex. They showed that the results of the DQM were in excellent agreement with the numerical forth-order Runge-Kutta solution.

Ghasemi *et al.* (2016a) applied the Differential Quadrature Method (DQM) to find an accurate solution for blood flow analysis in femoral and coronary arteries. They showed that the results of the DQM were in excellent agreement with the numerical Crank Nicholson Method (CNM).

Application of the Differential Quadrature Method (DQM) for boundary layer flow over a flat plate with slip flow and constant heat flux surface condition was studied by Moghimi *et al.* (2013). Wang (1988) studied the steady flow of a viscous and incompressible fluid outside of a stretching hollow cylinder in an ambient fluid at rest. Ishak *et al.* (2008) investigated the flow and heat transfer of a viscous and incompressible electrically conducting fluid outside of a stretching cylinder in the presence of a constant transverse magnetic field. The problem is governed by a third-order nonlinear ordinary differential equation that leads to exact similarity solutions of the Navier-Stokes equations.

The main aim of this paper is to simulate the problem of the flow of a nanofluid outside of a stretching cylinder in the presence of magnetic field by DQM and to compare the obtained results with those of Ishak *et al.* (2008), which represent the influence of adding nanoparticles to the base fluid. Also, the effects of some parameters such as the solid volume fraction of nanoparticles, type of the nanofluid and the magnetic parameter on velocity and temperature profiles are examined.

2. Formulation of the problem

Consider a steady laminar flow of an incompressible electrically conducting fluid (with electrical conductivity σ) caused by a stretching tube of radius a in the axial direction in the fluid at rest as shown in Fig. 1, where the z-axis is measured along the axis of the tube and the r-axis is measured in the radial direction. It is assumed that the surface of the tube is at constant

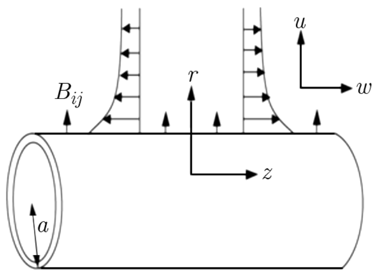

Fig. 1. Physical model and coordinate system

temperature T_w and the ambient fluid temperature is T_1, where $T_w > T_1$. We also assume that the uniform magnetic field of intensity B_0 acts in the radial direction and that the effect of the induced magnetic field is negligible, which is valid when the magnetic Reynolds number is small. The viscous dissipation, Ohmic heating and Hall effects are neglected as they are also assumed to be small. The fluid is a water based nanofluid containing different types of nanoparticles: Cu, Al_2O_3 and TiO_2. It is assumed that the base fluid and the nanoparticles are in thermal equilibrium and no slip occurs between them. The thermo physical properties of the nanofluid are given in Table 1

Table 1. Thermo-physical properties of water and nanoparticles (Oztop and Abu-Nada, 2008)

	ρ [kg/m^3]	C_p [J/(kgK)]	k [W/(mK)]	β [1/K]
Pure water	997.1	4179	0.613	21
Copper (Cu)	8933	385	401	1.67
Silver (Ag)	10500	235	429	1.89
Alumina (Al_2O_3)	3970	765	40	0.85
Titanium Oxide (TiO_2)	4250	686.2	8.9538	0.9

(see Oztop and Abu-Nada, 2008). On the above assumptions, the boundary layer equations governing the flow, and the concentration field can be written in dimensional form as

$$\begin{aligned}
&\frac{\partial(ru)}{\partial r} + \frac{\partial(rw)}{\partial z} = 0 \qquad u\frac{\partial w}{\partial r} + w\frac{\partial w}{\partial z} = \frac{\mu_{nf}}{\rho_{nf}}\Big(\frac{\partial^2 w}{\partial r^2} + \frac{1}{r}\frac{\partial w}{\partial r}\Big) - \frac{\sigma B_0^2}{\rho_{nf}}w \\
&u\frac{\partial u}{\partial r} + w\frac{\partial u}{\partial z} = -\frac{1}{\rho_{nf}}\frac{\partial p}{\partial r} + \frac{\mu_{nf}}{\rho_{nf}}\Big(\frac{\partial^2 u}{\partial r^2} + \frac{1}{r}\frac{\partial u}{\partial r} - \frac{u}{r^2}\Big) \\
&(\rho C_p)_{nf}\Big(w\frac{\partial T}{\partial z} + u\frac{\partial T}{\partial r}\Big) = k_{nf}\Big(\frac{\partial^2 T}{\partial r^2} + \frac{1}{r}\frac{\partial T}{\partial r}\Big)
\end{aligned} \tag{2.1}$$

Subject to the following boundary conditions

$$\begin{array}{llll} u = 0 & w = W_w & T = T_w & \text{at} \quad r = a \\ w \to 0 & T \to T_\infty & & \text{as} \quad r \to \infty \end{array} \tag{2.2}$$

where u and w are the velocity components along the r and z axes, respectively, $W_w = 2cz$ where c is a positive constant, and a is a constant. Further, ν, ρ, T and α are the kinematic viscosity, fluid density, fluid temperature and thermal diffusivity, respectively. It is necessary to mention that the magnetic term in Eq. $(2.1)_3$ (in the r direction) is neglected because it does not affect the flow dynamics in perpendicular situations and can be absorbed by the pressure term.

The effective density ρ_{nf}, the effective dynamic viscosity μ_{nf}, the heat capacitance $(\rho Cp)_{nf}$ and the thermal conductivity k_{nf} of the nanofluid are given as (see Aminossadati and Ghasemi, 2009)

$$\begin{array}{ll} (\rho C_p)_{nf} = (\rho C_p)_f(1-\varphi) + (\rho C_p)_s\varphi & \dfrac{k_{nf}}{k_f} = \dfrac{k_s + 2k_f - 2\varphi(k_f - k_s)}{k_s + 2k_f + \varphi(k_f - k_s)} \\ \rho_{nf} = \rho_f(1-\varphi) + \rho_s\varphi & \mu_{nf} = \dfrac{\mu_f}{(1-\varphi)^{2.5}} \end{array} \tag{2.3}$$

Here, φ is the solid volume fraction, μ_f is the dynamic viscosity of the basic fluid, ρ_f and ρ_s are the densities of the pure fluid and nanoparticle, respectively. $(\rho C_p)_f$ and $(\rho C_p)_s$ are the specific heat parameters of the base fluid and nanoparticle, k_f and k_s are the thermal conductivities of the base fluid and nanoparticle, respectively. Following Wang (1988), we take the similarity transformation

$$u = -ca\frac{f(\eta)}{\sqrt{\eta}} \qquad w = 2cf'(\eta)z \qquad \eta = \Big(\frac{r}{a}\Big)^2 \qquad \theta = \frac{T - T_\infty}{T_w - T_\infty} \tag{2.4}$$

where the prime denotes differentiation with respect to η. Substituting Eq. (14) into Eqs. $(2.1)_2$ and $(2.1)_4$, we get the following ordinary differential equations

$$\begin{array}{l} \dfrac{1}{(1-\varphi)^{2.5}}\dfrac{1}{1-\varphi+\frac{\rho_s}{\rho_f}\varphi}(f'''\eta + f'') - \dfrac{M}{1-\varphi+\frac{\rho_s}{\rho_f}\varphi}f' - \mathrm{Re}f'^2 + \mathrm{Re}ff'' = 0 \\ \theta''\eta + \theta' + f\theta'\mathrm{Re}\,\mathrm{Pr}\,\dfrac{1-\varphi+\frac{(\rho C_p)_s}{(\rho C_p)_f}\varphi}{\frac{k_s+2k_f-2\varphi(k_f-k_s)}{k_s+2k_f+\varphi(k_f-k_s)}} = 0 \end{array} \tag{2.5}$$

where $\mathrm{Re} = ca^2/(2\nu_{nf})$ is the Reynolds number and $M = \sigma B_0^2a^2/(4\nu_{nf}\rho_{nf})$ is the magnetic parameter. ν_{nf} is the kinematic viscosity of nanofluid. Boundary conditions (2.2) become

$$\begin{array}{lll} f(1) = 0 & f'(1) = 1 & \theta(1) = 1 \\ f(\infty) \to 0 & \theta(\infty) \to 0 & \end{array} \tag{2.6}$$

The pressure can now be determined from Eq. $(2.1)_3$ in the following form

$$\frac{p - p_\infty}{\rho cv} = -\frac{\mathrm{Re}}{\eta}f^2(\eta) - 2f'(\eta) \tag{2.7}$$

The physical quantities of interest are the skin friction coefficient and the Nusselt number, which are defined as follows

$$C_f = \frac{\tau_w}{\rho W_w/2} \qquad \mathrm{Nu} = \frac{aq_w}{k(T_w - T_\infty)} \tag{2.8}$$

Furthermore, τ_w and q_w are the skin friction and the heat transfer from the surface of the tube, respectively, and are given as

$$\tau_w = \mu\Big(\frac{\partial w}{\partial r}\Big)_{r=a} \qquad q_w = -k\Big(\frac{\partial T}{\partial r}\Big)_{r=a} \tag{2.9}$$

where k is the thermal conductivity. Considering variables (2.4), we get

$$C_f\frac{\mathrm{Re}z}{a} = f''(1) \qquad \mathrm{Nu} = -2\theta'(1) \tag{2.10}$$

3. Differential Quadrature Method (DQM)

The differential qquadrature method (DQM) is a rather efficient numerical method for rapid solution of linear and nonlinear partial differential equations (Bellman *et al.*, 1972). Compared with the conventional methods such as the finite element and finite difference methods, the DQM requires less computer time and storage.

In this study, a polynomial expansion based differential quadrature, as introduced by Quan and Chang (1989), is applied for solving the problem. Several attempts have been made by researchers to develop polynomial based differential quadrature methods. One of the most useful approaches is the one that uses the following Lagrange interpolation polynomials as test functions

$$g_k = \frac{M(x)}{(x-x_k)M^{(1)}(x_k)} \qquad k = 1,2,\dots,N \tag{3.1}$$

where

$$M(x) = (x-x_1)(x-x_2)\cdots(x-x_N) \qquad M^{(1)}(x_i) = \prod_{\substack{k=1\\k\neq i}}^{N}(x_i-x_k) \tag{3.2}$$

By applying the above equation at N grid points, the following algebraic formulations to compute the weighting coefficients are developed

$$\begin{aligned} &A_{ij}^{(1)} = \frac{1}{x_j-x_i}\prod_{\substack{k=1\\k\neq i,j}}^{N}\frac{x_i-x_k}{x_j-x_k} \qquad i\neg j\\ &A_{ij}^{(1)} = \sum_{\substack{k=1\\k\neq i}}^{N}\frac{1}{x_i-x_k} \qquad A_{ij}^{(2)} = \sum_{k=1}^{N}A_{ik}^{(1)}A_{kj}^{(1)} \end{aligned} \tag{3.3}$$

where $A^{(1)}$ and $A^{(2)}$ denote the weighting coefficients of the first and second order derivatives of the function $f(r)$ with respect to the r direction. N is the number of grid points chosen in the r direction. The differential quadrature approximation can be easily extended from the above formulation to other coordinates. The first order derivatives in the two-dimensional formulation are approximated by

$$\frac{\partial f}{\partial r}\Big|_{ij} \approx \sum_{l=1}^{N}A_{il}^{(1)}f_{lj} \qquad \frac{\partial f}{\partial z}\Big|_{ij} \approx \sum_{m=1}^{M}B_{jm}^{(1)}f_{im} \tag{3.4}$$

And the second order derivatives can be approximated by:

$$
\begin{aligned}
&\left.\frac{\partial f}{\partial r}\right|_{ij} \approx \sum_{l=1}^{N} A_{il} f_{lj} \qquad &&\left.\frac{\partial^2 f}{\partial r^2}\right|_{ij} \approx \sum_{l=1}^{N} A_{il}^{(2)} f_{lj}\\
&\left.\frac{\partial f}{\partial z}\right|_{ij} \approx \sum_{m=1}^{P} B_{jm} f_{im} \qquad &&\left.\frac{\partial^2 f}{\partial z^2}\right|_{ij} \approx \sum_{n=1}^{P} B_{kn}^{(2)} f_{ijn}\\
&\left.\frac{\partial^2 f}{\partial r \partial z}\right|_{ij} \approx \sum_{l=1}^{N} A_{il}^{(1)} \sum_{m=1}^{P} B_{jm}^{(1)} f_{lm}
\end{aligned}
\tag{3.5}
$$

where $A^{(1)}$ and $B^{(1)}$ denote the weighting coefficients of the first order derivatives; $A^{(2)}$ and $B^{(2)}$ denote the weighting coefficients of the second order derivatives of the function $f(r, z)$ with respect to the r and z-directions, respectively; N and P are the number of grid points chosen in the r and z-directions, respectively.

4. Results and discussion

Equations (2.5) along with their boundary conditions are solved numerically by using the DQM. After applying this method, the influence of several non-dimensional parameters, namely the Reynolds number Re, Prandtl number Pr, nanoparticles volume fraction φ and magnetic parameter M, have been investigated. Validating the numerical results obtained in this study, the case when the volume fraction coefficient is zero ($\varphi = 0$) has been considered and compared with the previously published results in Tables 2 and 3. These tables present numerical values of the skin friction coefficient in terms of $f''(1)$ and the Nusselt number Nu in terms of $-\theta'(1)$ along with the results reported by Ishak *et al.* (2008), which show an excellent agreement with the achieved results in the present study.

Table 2. Values of the skin friction coefficient for several values of M and Re at Pr = 6.2

M	Re = 1		Re = 5	
	Present work	Ishak *et al.* (2008)	Present work	Ishak *et al.* (2008)
0	−1.17849	−1.1780	−2.41745	−2.4174
0.01	−1.18431	−1.1839	−2.41990	−2.4199
0.05	−1.20708	−1.2068	−2.42965	−2.4296
0.10	−1.23454	−1.2344	−2.44174	−2.4417
0.50	−1.42693	−1.4269	−2.53523	−2.5352

Table 3. Values of the Nusselt number for several values of M and Re at Pr = 6.2

M	Re = 1		Re = 5	
	Present work	Ishak *et al.* (2008)	Present work	Ishak *et al.* (2008)
0	2.05857	2.0587	19.1185	19.1587
0.01	2.05715	2.0572	19.1184	19.1586
0.05	2.05158	2.0516	19.1179	19.1581
0.10	2.04487	2.0449	19.1174	19.1576
0.50	1.99806	1.9978	19.1129	19.1530

Figure 2 shows the effect of volume fraction coefficient φ on velocity distribution for Re = 5. It is noticed that the Prandtl number Pr gives no effect to the velocity as can be seen from

Eq. $(2.5)_1$. The velocity curves show that the rate of transport is considerably reduced with an increase of φ. In all cases, the velocity vanishes at some large distance from the surface of the tube.

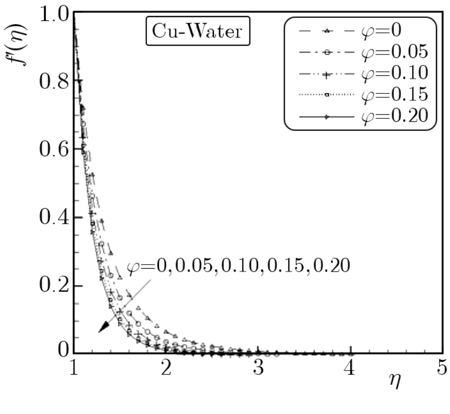

Fig. 2. Velocity profiles for various values of φ (Re $= 5$, $M = 5$, Pr $= 6.2$)

Figure 3 presents temperature profiles for various values of φ when Pr $= 6.2$ and Re $= 5$, and the nanoparticle is Cupper. It is obvious that the temperature increases as φ increases, but it decreases as the distance from the surface increases, and finally vanishes at a some large distance from the surface. Consider that $\varphi = 0$ represents pure water like what is presented by Ishak *et al.* (2008). It is clear that the heat transfer in the present case is more than the case when the fluid is pure water.

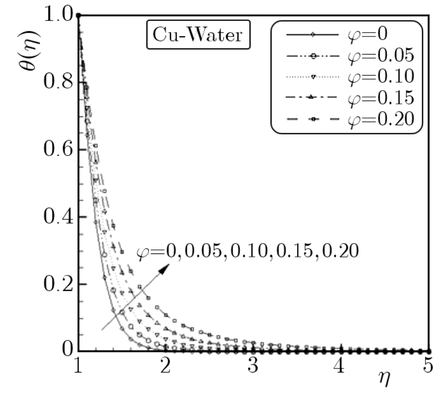

Fig. 3. Temperature profiles for various values of φ (Re $= 5$, $M = 5$, Pr $= 6.2$)

Figure 4a exhibits the skin friction coefficient profiles C_f for various values of the Reynolds number Re as M is constant. It is observed that the magnitude of the skin friction coefficient increases as Re increases. Figure 4b represents the skin friction coefficient profiles C_f for various values of M when the Reynolds number Re is constant. It can be seen that the magnitude of the skin friction coefficient grows as M increases.

Furthermore, it is clear from both Figs. 4a,b that the skin friction coefficient increases with an increase in the volume fraction coefficient. The same behavior can be observed for the Nusselt number, i.e. growing Re increases the temperature gradient and, in turn, increases the Nusselt number. And an increase in M decreases the Nusselt number, which is obvious from Figs. 5a,b. Also, it is clear that the Nusselt number increases with an increase in the volume friction coefficient.

After the velocity $f'(\eta)$ is obtained, the pressure p in terms of $(p - p_\infty)/(\rho cv)$ can be found by using Eq. (2.7). The numerical results are shown in Fig. 6a for $M = 2$, $\varphi = 0.1$ and Re $= 1$, 5

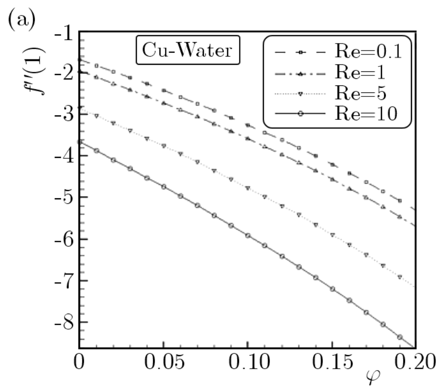

Fig. 4. Skin friction coefficient for various values of (a) Re and φ ($M = 2$, $\mathrm{Pr} = 6.2$), (b) M and φ ($\mathrm{Re} = 5$, $\mathrm{Pr} = 6.2$)

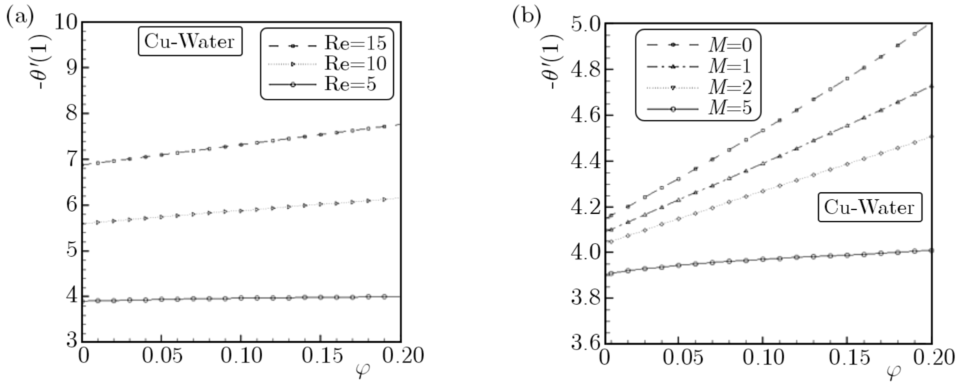

Fig. 5. Nusselt number for various values of (a) Re and φ ($M = 2$, $\mathrm{Pr} = 6.2$), (b) M and φ ($\mathrm{Re} = 5$, $\mathrm{Pr} = 6.2$)

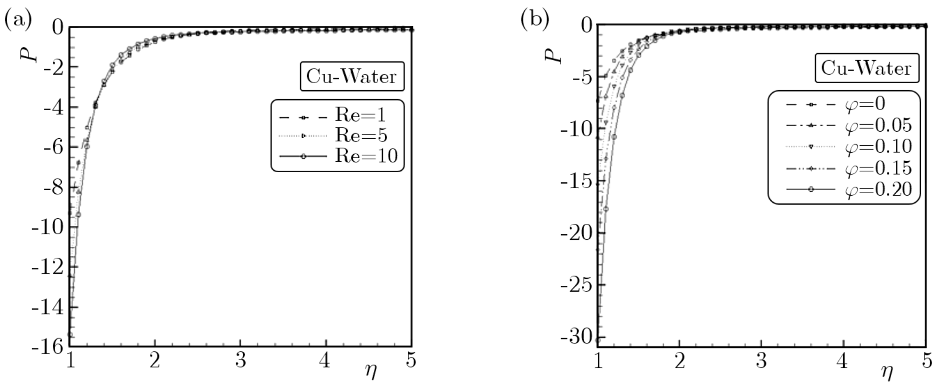

Fig. 6. Pressure distribution obtained from Eq. (2.7) for various values of (a) Re ($\varphi = 0.1$, $M = 2$, $\mathrm{Pr} = 6.2$), (b) φ ($\mathrm{Re} = 10$, $M = 2$, $\mathrm{Pr} = 6.2$)

and 10. All curves show that $p \to p_\infty$ far away from the surface $\eta \to \infty$. Further, Fig. 6b shows the pressure curve for different values of φ when $\mathrm{Re} = 10$ and $M = 2$. It is clear from this figure that bigger values of φ result in slower algebraic decay. In other words, if $\varphi = 0.2$, sufficient decay of $(p - p_\infty)$ takes place at higher values of η than the case when $\varphi = 0$.

Figures 7a and 7b represent $f'(\eta)$ and $\theta(\eta)$ curves, respectively, for different types of nanoparticles, namely, Cu, Al_2O_3 and TiO_2 when $\varphi = 0.1$, $M = 5$, $\mathrm{Pr} = 6.2$, and $\mathrm{Re} = 5$. The figure shows that by using different types of nanofluids, values of the velocity and temperature change, i.e. we can say that the sheer stress and the rate of hate transfer change by using different types of nanofluids. This means that the nanofluids will be important in the cooling and heating processes.

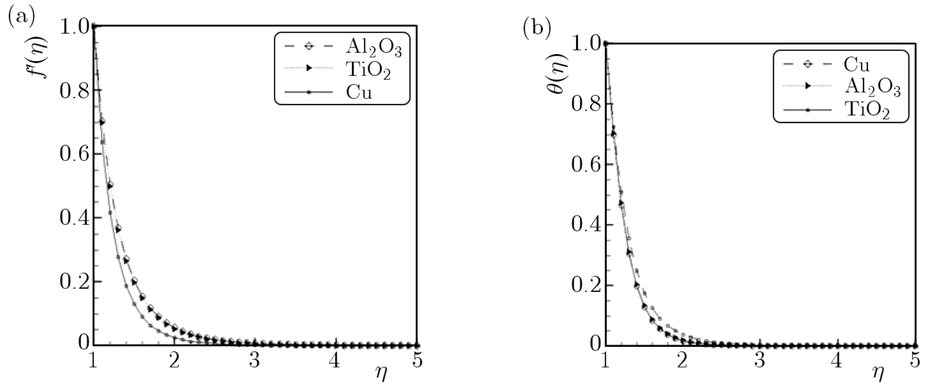

Fig. 7. (a) Velocity profiles and (b) temperature profiles for various values of nonoparticles ($\varphi = 0.1$, $\mathrm{Re} = 5$, $M = 5$, $\mathrm{Pr} = 6.2$)

5. Conclusions

A steady two dimensional flow of an electrically conducting incompressible nanofluid due to stretching cylindrical tube is studied in the present work. Similarity solutions are obtained for a linearly stretching tube with a constant surface temperature, and the achieved ordinary differential equations are solved numerically by applying the Differential Quadrature Method (DQM). Effects of the volume fraction coefficient, magnetic parameter and Reynolds number on the flow and heat transfer characteristics have been examined. It can be concluded that the magnitude of the skin friction coefficient increases with the volume fraction coefficient, magnetic parameter and Reynolds number, while it is constant with the Prandtl number. The Nusselt number, also, increases with the volume fraction coefficient and Reynolds number but decreases with the magnetic parameter.

References

1. Aminossadati S.M., Ghasemi B., 2009, Natural convection cooling of a localised heat source at the bottom of a nanofluid-filled enclosure, *European Journal of Mechanics – B/Fluids*, **28**, 630-640

2. Atouei S.A., Hosseinzadeh Kh., Hatami M., Ghasemi Seiyed E., Sahebi S.A.R., Ganji D.D., 2015, Heat transfer study on convectiveeradiative semi-spherical fins with temperature-dependent properties and heat generation using efficient computational methods, *Applied Thermal Engineering*, **89**, 299-305

3. Bellman R.E., Kashef B.G., Casti J., 1972, Differential quadrature: A technique for the rapid solution of nonlinear partial differential equations, *Journal of Computational Physics*, **10**, 40-52

4. Choi S.U.S., 1995, Enhancing thermal conductivity of fluids with nanoparticles, *ASME Fluids Engineering Division*, **231**, 99-105

5. Darzi M., Vatani M., Ghasemi S.E., Ganji D.D., 2015, Effect of thermal radiation on velocity and temperature fields of a thin liquid film over a stretching sheet in a porous medium, *European Physical Journal Plus*, **130**, 100

6. Ghasemi S.E., Hatami M., Ganji D.D., 2013, Analytical thermal analysis of air-heating solar collectors, *Journal of Mechanical Science and Technology*, **27**, 11, 3525-3530

7. Ghasemi S.E., Hatami M., Ganji D.D., 2014a, Thermal analysis of convective fin with temperature-dependent thermal conductivity and heat generation, *Case Studies in Thermal Engineering*, **4**, 1-8

8. Ghasemi S.E., Hatami M., Hatami J., Sahebi S.A.R., Ganji D.D., 2016a, An efficient approach to study the pulsatile blood flow in femoral and coronary arteries by Differential Quadrature Method, *Physica A*, **443**, 406-414

9. Ghasemi S.E., Hatami M., Kalani Sarokolaie A., Ganji D.D., 2015a, Study on blood flow containing nanoparticles through porous arteries in presence of magnetic field using analytical methods, *Physica E*, **70**, 146-156

10. Ghasemi S.E., Hatami M., Mehdizadeh Ahangar GH.R., Ganji D.D., 2014b, Electrohydrodynamic flow analysis in a circular cylindrical conduit using Least Square Method, *Journal of Electrostatics*, **72**, 47-52

11. Ghasemi S.E., Jalili Palandi S., Hatami M., Ganji D.D., 2012, Efficient analytical approaches for motion of a spherical solid particle in plane couette fluid flow using nonlinear methods, *The Journal of Mathematics and Computer Science*, **5**, 2, 97-104

12. Ghasemi S.E., Valipour P., Hatami M., Ganji D.D., 2014c, Heat transfer study on solid and porous convective fins with temperature-dependent heat generation using efficient analytical method, *Journal of Central South University*, **21**, 4592-4598

13. Ghasemi S.E., Vatani M., Ganji D.D., 2015b, Efficient approaches of determining the motion of a spherical particlein a swirling fluid flow using weighted residual methods, *Particuology*, **23**, 68-74

14. Ghasemi S.E., Vatani M., Hatami M., Ganji D.D., 2016b, Analytical and numerical investigation of nanoparticles effect on peristaltic fluid flow in drug delivery systems, *Journal of Molecular Liquids*, **215**, 88-97

15. Ghasemi S.E., Zolfagharian A., Ganji D.D., 2014d, Study on motion of rigid rod on a circular surface using MHPM, *Propulsion and Power Research*, **3**, 3, 159-164

16. Ghasemi S.E., Zolfagharian A., Hatami M., Ganji D.D., 2015c, Analytical thermal study on nonlinear fundamental heat transfer cases using a novel computational technique, *Applied Thermal Engineering*, http://dx.doi.org/10.1016/j.applthermaleng.2015.11.120

17. Harada N., Tsunoda K., 1998, Study of a disk MHD generator for nonequilibrium plasma generator (NPG) system, *Energy Conversion and Management*, **39**, 493-503

18. Hatami M., Ganji D.D., 2014, Motion of a spherical particle in a fluid forced vortex by DQM and DTM, *Particuology*, **16**, 206-212

19. Hatami M., Ghasemi S.E., Sahebi S.A.R., Mosayebidorcheh S., Ganji D.D., Hatami J., 2015d, Investigation of third-grade non-Newtonian blood flow in arteries under periodic body acceleration using multi-step differential transformation method, *Applied Mathematics and Mechanics*, **36**, 11, 1449-1458

20. Ho C.J., Chen M.W., Li Z.W., 2008, Numerical simulation of natural convection of nanofluid in a square enclosure: effects due to uncertainties of viscosity and thermal conductivity, *International Journal of Heat and Mass Transfer*, **51**, 4506-4516

21. Ishak A., Nazar R., Pop I., 2006, Magnetohydrodynamic stagnation-point flow towards a stretching vertical sheet, *Magnetohydrodynamics*, **42**, 17-30

22. Ishak A., Nazar R., Pop I., 2008, Magnetohydrodynamic (MHD) flow and heat transfer due to a stretching cylinder, *Energy Conversion and Management*, **49**, 3265-3269

23. Magyari E., Keller B., 1999, Heat and mass transfer in the boundary layers on an exponentially stretching continuous surface, *Journal of Physics D: Applied Physics*, **32**, 577-585

24. Mahapatra T.R., Gupta A.S., 2001, Magnetohydrodynamic stagnation-point flow towards a stretching sheet, *Acta Mechanica*, **152**, 191-196

25. Misagh Imani S., Goudarzi A.M., Ghasemi S.E., Kalani A., Mahdinejad J., 2014, Analysis of the stent expansion in a stenosed artery using finite element method: Application to stent versus stent study, *Proceedings of the Institution of Mechanical Engineers, Part H: Journal of Engineering in Medicine*, **228**, 10, 996-1004

26. Moghimi M.A., Tabaei H., Kimiaeifar A., 2013, HAM and DQM solutions for slip flow over a flat plate in the presence of constant heat flux, *Mathematical and Computer Modelling*, **58**, 1704-1713

27. Moghimi M.A., Talebizadeh P., Mehrabian M.A., 2011, Heat generation/absorption effects on magnetohydrodynamic natural convection flow over a sphere in a non-Darcian porous medium, *Proceedings of the Institution of Mechanical Engineers, Part E: Journal of Process Mechanical Engineering*, **225**, 29-39

28. Mohammadian E., Ghasemi S.E., Poorgashti H., Hosseini M. and Ganji D.D., 2015, Thermal investigation of Cu-water nanofluid between two vertical planes, *Proceedings of the Institution of Mechanical Engineers, Part E: Journal of Process Mechanical Engineering*, **229**, 1, 36-43

29. Oztop H.F., Abu-Nada E., 2008, Numerical study of natural convection in partially heated rectangular enclosures filled with nanofluids, *International Journal of Heat and Fluid Flow*, **29**, 1326-1336

30. Quan J.R., Chang C.T., 1989, New insights in solving distributed system equations by quadrature methods – I. Analysis, *Computers and Chemical Engineering*, **13**, 779-788

31. Shang J.S., 2001, Recent research in magneto-aerodynamics, *Progress in Aerospace Sciences*, **37**, 1-20

32. Shu C., 2000, *Differential Quadrature and its Application in Engineering*, Springer

33. Talebizadeh P., Moghimi M.A., Kimiaeifar A., Ameri M., 2011, Numerical and analytical solution for natural convection flow with thermal radiation and mass transfer past a moving vertical porous plate by DQM and HAM, *International Journal of Computational Methods*, **8**, 611-631

34. Valipour P., Ghasemi S.E., Vatani M., 2015, Theoretical investigation of micropolar fluid flow between two porous disks, *Journal of Central South University*, **22**, 2825-2832

35. Vatani M., Ghasemi S.E., Ganji D.D., 2014, Investigation of micropolar fluid flow between a porous disk and a nonporous disk using efficient computational technique, *Proceedings of the Institution of Mechanical Engineers, Part E: Journal of Process Mechanical Engineering*, DOI:10.1177/0954408914557375

36. Wang C.Y., 1988, Fluid flow due to a stretching cylinder, *Physics of Fluids*, **31**, 466-468

37. Ziabakhsh Z., Domairry G., Mozaffari M., Mahbobifar M., 2010, Analytical solution of heat transfer over an unsteady stretching permeable surface with prescribed wall temperature, *Journal of the Taiwan Institute of Chemical Engineers*, **41**, 169-177

38. Ziabakhsh Z., Domairry G., 2009, Solution of the laminar viscous flow in a semi-porous channel in the presence of a uniform magnetic field by using the homotopy analysis method, *Communications in Nonlinear Science and Numerical Simulation*, **14**, 1284-1294

39. Zolfagharian A., Ghasemi S.E., Misagh I., 2014a, A multi-objective, active fuzzy force controller in control of flexible wiper system, *Latin American Journal of Solids and Structures*, **11**, 9, 1490-1514

40. Zolfagharian A., Noshadi A., Ghasemi S.E., Md. Zain M.Z., 2014b, A nonparametric approach using artificial intelligence in vibration and noise reduction of flexible systems, *Proceedings of the Institution of Mechanical Engineers, Part C, Journal of Mechanical Engineering Science*, **228**, 8, 1329-1347

41. Zolfagharian A., Noshadi A., Khosravani M.R., Md. Zain M.Z., 2014c, Unwanted noise and vibration control using finite element analysis and artificial intelligence in flexible wiper system, *Applied Mathematical Modelling*, **38**, 2435-2453

42. Zolfagharian A., Valipour P., Ghasemi S.E., 2015, Fuzzy force learning controller of flexible wiper system, *Neural Computing and Application*, **26**, 2, DOI: 10.1007/s00521-015-1869-0

Manuscript received October 25, 2014; accepted for print September 15, 2015